



Supplement of

Tracing differences in iron supply to the Mid-Atlantic Ridge valley between hydrothermal vent sites: implications for the addition of iron to the deep ocean

Alastair J. M. Lough et al.

Correspondence to: Alastair J. M. Lough (a.j.m.lough@leeds.ac.uk)

The copyright of individual parts of the supplement might differ from the article licence.

Contents of this file

**Supplementary Table S1 and S2
Supplementary Figures S1 to S11**

Table S1. Extended summary of plume dFe/xs³He ratios over vent sites and for repeat sampling at TAG and Rainbow using different methods to calculate dFe/xs³He. The young rising plume was identified over Rainbow as a narrow spike in depth profiles of TDFe, dFe, xs³He and dMn close to the seafloor (Supplementary Information, Figure S8). This signal is separated as these samples will be from a cross section of the young rising plume as the CTD rosette passed through it.

Site (station)	Plume-integrated dFe/xs ³ He (nmole/fmole)		dFe/xs ³ He (nmole/fmole) from the slope of regression	
	Integrated from separate casts (Method 1)	Dual-Mn method (Method 2)	Interpolation method (Method 3)	
			slope	r ²
Menez Gwen (6)	5.35	11.8	6.12	1.00
Lucky Strike (7)	25.8	4.17	-10.1	0.901
Lucky Strike (8)	ND	7.92	ND	
Rainbow (16)	48.6	12.3	132	0.233
Rainbow (38)	35.5	43.6	-197	0.997
Rainbow* (38)	63.0	4.39	ND	
TAG (34)	4.36	7.37	0.10	0.003
TAG (35)	87.0	85.6	113	0.538
TAG (37)	ND	3.60	ND	
Close E Rainbow 33 km (12)	5.43	4.12	14.6	0.479
Close W Rainbow 30 km (13)	8.24	7.55	9.88	0.132
Close N Rainbow 34 km (14)	14.7	8.33	-6.50	1.00
S of Rainbow 39 km (15)	10.6	6.08	11.6	0.099
Close S of Rainbow 10 km (17)	ND	5.83	ND	
N of Rainbow 25 km (18)	20.2	14.8	-16.2	-0.128
Close N of TAG 29 km (26)	ND	8.92	31.1	0.101
Close S of TAG 30 km (27)	ND	4.25	-0.88	-0.140
Close W of TAG 30 km (30)	29.8	37.5	512	-0.211
Close E of TAG 30 km (31)	ND	3.88	-7.75	-0.270
Close N of TAG 18 km (36)	ND		25.9	0.416

ND = no data, either no dMn data available from the trace metal rosette or no ³He data available from the standard rosette at the equivalent depth. Site with an r² of 1.00 indicate only 2 samples fit the plume criteria for regression after data was re-gridded.

*The young rising plume was identified over Rainbow close to the seafloor with density lower than that of other stations at the same depth (Supplementary Information, Figure S8 and S10). This signal is separated as these samples will be from a cross section of the young rising plume as the CTD rosette passed through it).

xs³He interpolation method: Interpolates the distinct dFe and xs³He data in a depth profile to create a matchup between both variables to calculate the dFe/xs³He using linear regression (Saito et al., 2013). This assumes that any change in concentration between sampled depths is linear and with no additional sources of variability. Note that Saito et al. (2013) did not measure xs³He but used data from a separate cruise then interpolated across xs³He sampling depths from the separate cruise data to match dFe sample depths and location. Saito et al. (2013) account for differences in water mass distribution between separate casts on separate cruises using optimum multi-parameter analysis. We did not do any correction for differences in water masses when using this interpolation method as our separate casts were typically taken within 24 hours of each other so there was minimal if any change in basin scale water mass contributions with depth.

The estimated ratios from interpolation are so significantly different from the other two methods of estimation. Often producing negative values with a poor r² lower than 0.2. Differences between the xs³He interpolation method and the other two methods are largely because of the variability introduced by the interpolation method (often producing negative dFe/xs³He ratios) as the shape of the plume depth profile (for both xs³He and dFe) is not reproducible between trace metal clean and standard sampling casts (Figure 2, Figure S2 and S4) at the high spatial sampling resolution of this study. The xs³He interpolation method can only be used in an off-axis setting where it is safe to assume that the shape of xs³He and dFe depth profiles will not change between sampling casts, and therefore xs³He data can be transferred to dFe sampling depths or vice versa.

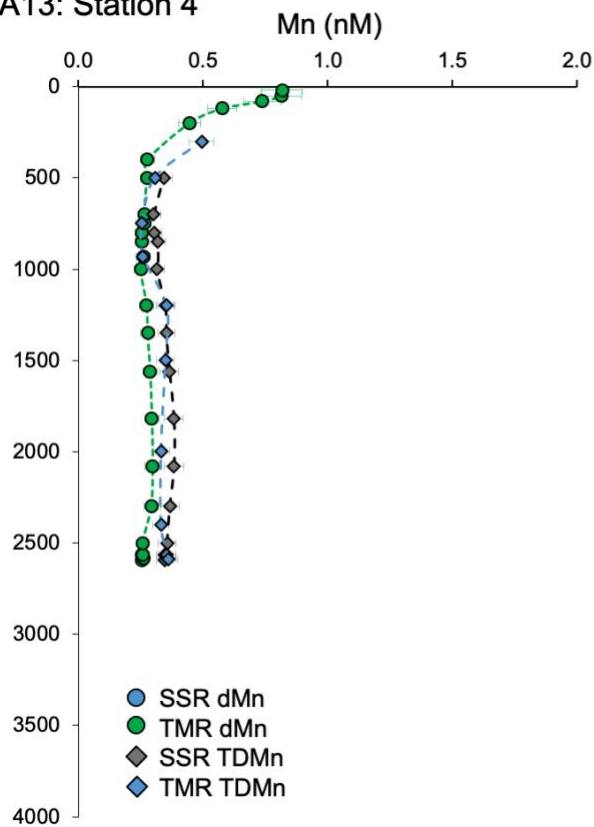
Table S2. Approximate diameters of Fe oxyhydroxide bearing particles from published studies on hydrothermal plumes (see main text for references)

Diameter (μm)	Scientific Study (first author, year)
0.735	Feeley 1994
10	Breier 2014
4	Breier 2014
6	Lough 2019 CG
1	Lough 2019 CG
5	Lough 2019 CG
1	Lough 2019 CG
1	Lough 2019 CG
4	Frontiers Lough 2019
10	Frontiers Lough 2019
2	Frontiers Lough 2019
1	Frontiers

	Lough 2019
3	Frontiers
	Lough 2019
6	Frontiers
	Lough 2017
12	GCA
	Lough 2017
18	GCA
	Lough 2017
24	GCA
	Lough 2017
6	GCA
	Lough 2017
20	GCA
	Toner 2016
10	Toner 2016
	Toner 2016
8	Toner 2016
	Toner 2009
5	Toner 2009
0.5	Toner 2009
	Von der Heyden
12	2012
<hr/>	
6.5	<i>average</i>
6.3	<i>St.dev</i>
28	<i>n</i>

Figures

GA13: Station 4



GA13: Station 25

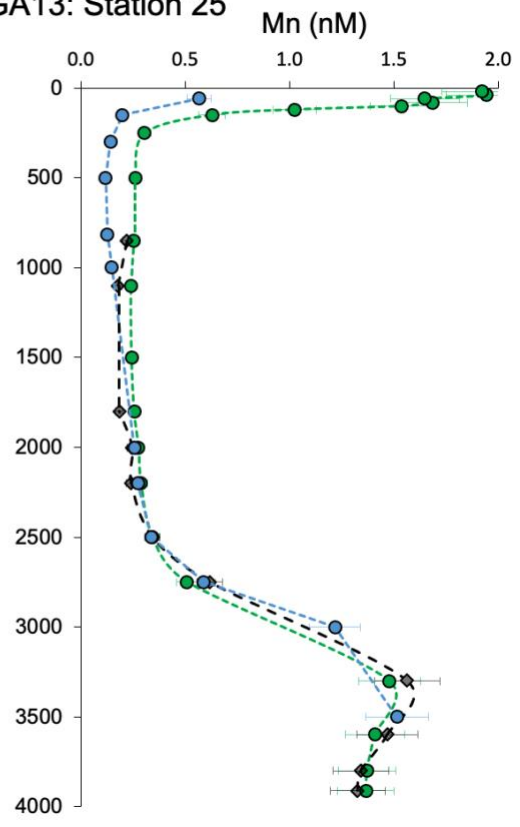


Figure S1. Comparison of dissolved and total dissolvable Mn data between the standard stainless steel (SSR) and trace metal clean (TMR) Niskin rosettes. Overlap of profiles indicates Mn can be sampled cleanly from the stainless-steel rosette without risk of contamination, as can be seen from these profiles with similar Mn concentrations to background N. Atlantic seawater. In this example all samples were measured by flow injection. We note a ~ 0.2 nM discrepancy between dMn measurements in surface waters at station 25 however this is unlikely to impact our assessment of the data which excludes samples shallower than 600 m. This ~ 0.2 nM difference in surface water could be a result of the time of day between casts or other factors rather than purely analytical variability.

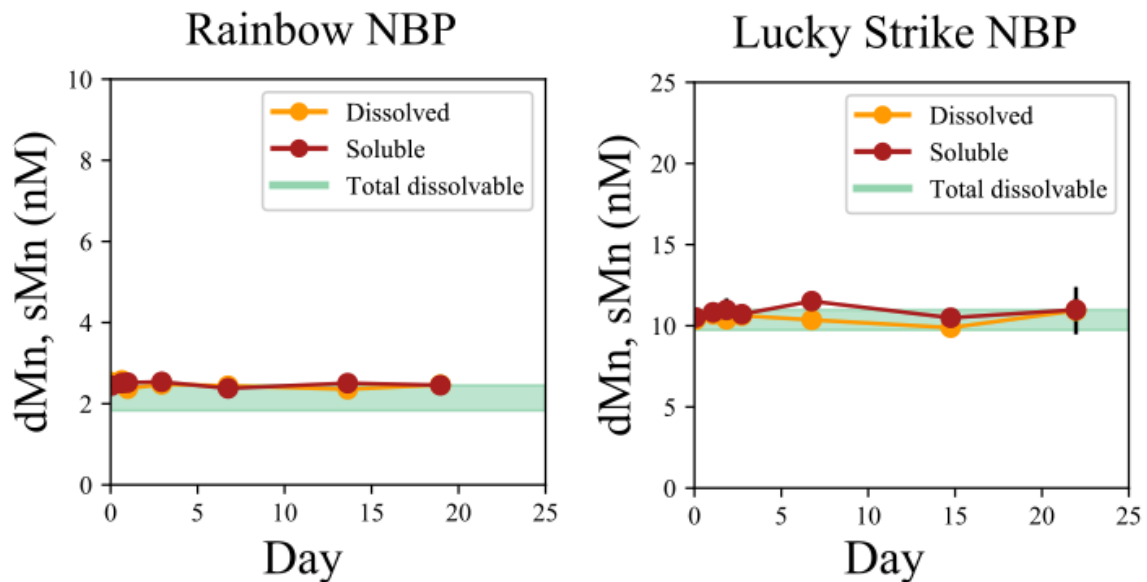


Figure S2. Dissolved, soluble, and total dissolvable manganese (Mn) concentrations in an incubation experiment on Rainbow and Lucky Strike unfiltered neutrally buoyant plume waters. Presented are the soluble ($<0.02 \mu\text{m}$) fraction (red circles) and dissolved ($<0.2 \mu\text{m}$) fraction (yellow circles) concentrations for Mn. The green band represents the average \pm the standard deviation of all total dissolvable (unfiltered, acidified) from every sample taken in the incubation. The constant dMn concentration through the incubation demonstrate that dMn is conservative within the time frame that it takes plume water to escape the ridge valley (Vic et al., 2018). Data are taken from Mellett et al. (in prep)

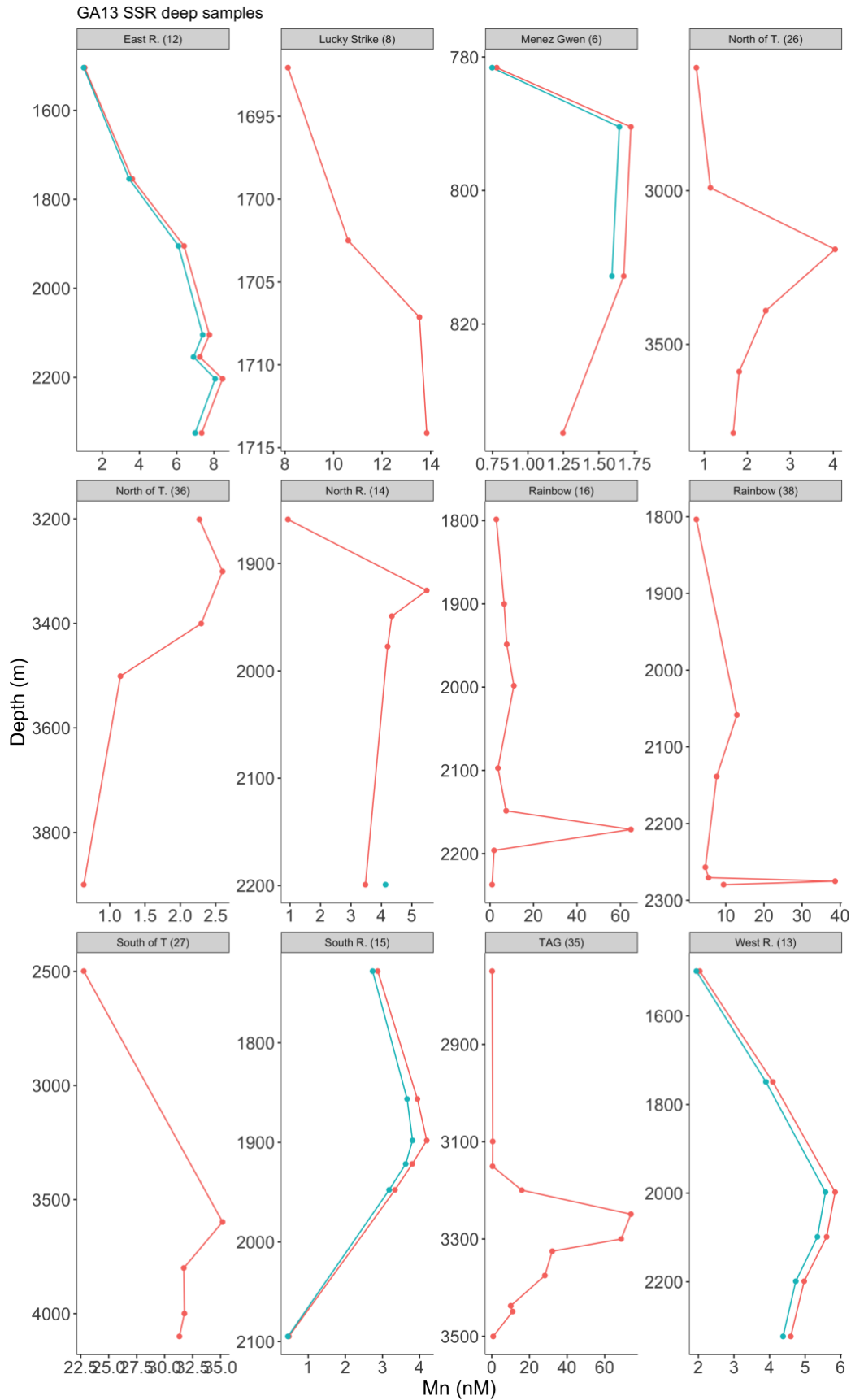


Figure S3. Dissolved Mn data (red) from the standard (stainless-steel) rosette at each station (grey box's), where dMn (red) >0.15 nM N. Atlantic background value and neutral density >27 mg/kg. Main casts over vent sites are 6 = Menez Gwen, 8 = Lucky Strike, 16 and 38 = Rainbow, 35 and 36 = TAG. Blue points show TDMn data measured and found to be within analytical uncertainty of dMn measurements.

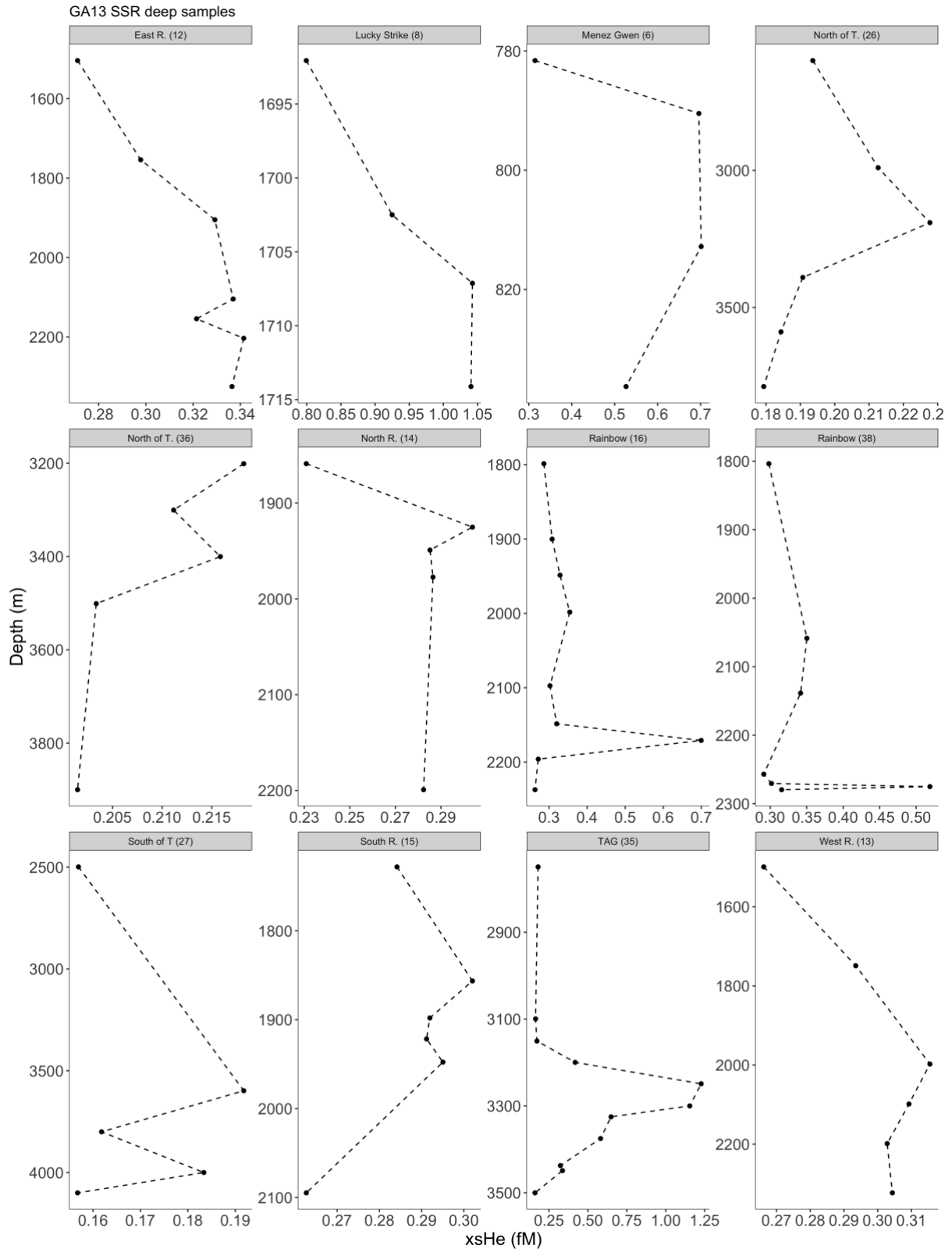


Figure S4. $xs^3\text{He}$ data from the stainless-steel rosette at each station (grey box's), where $dMn > 0.15$ nM N. Atlantic background value and neutral density > 27 mg/kg. Main casts over vent sites are 6 = Menez Gwen, 8 = Lucky Strike, 16 and 38 = Rainbow, 35 and 36 = TAG.

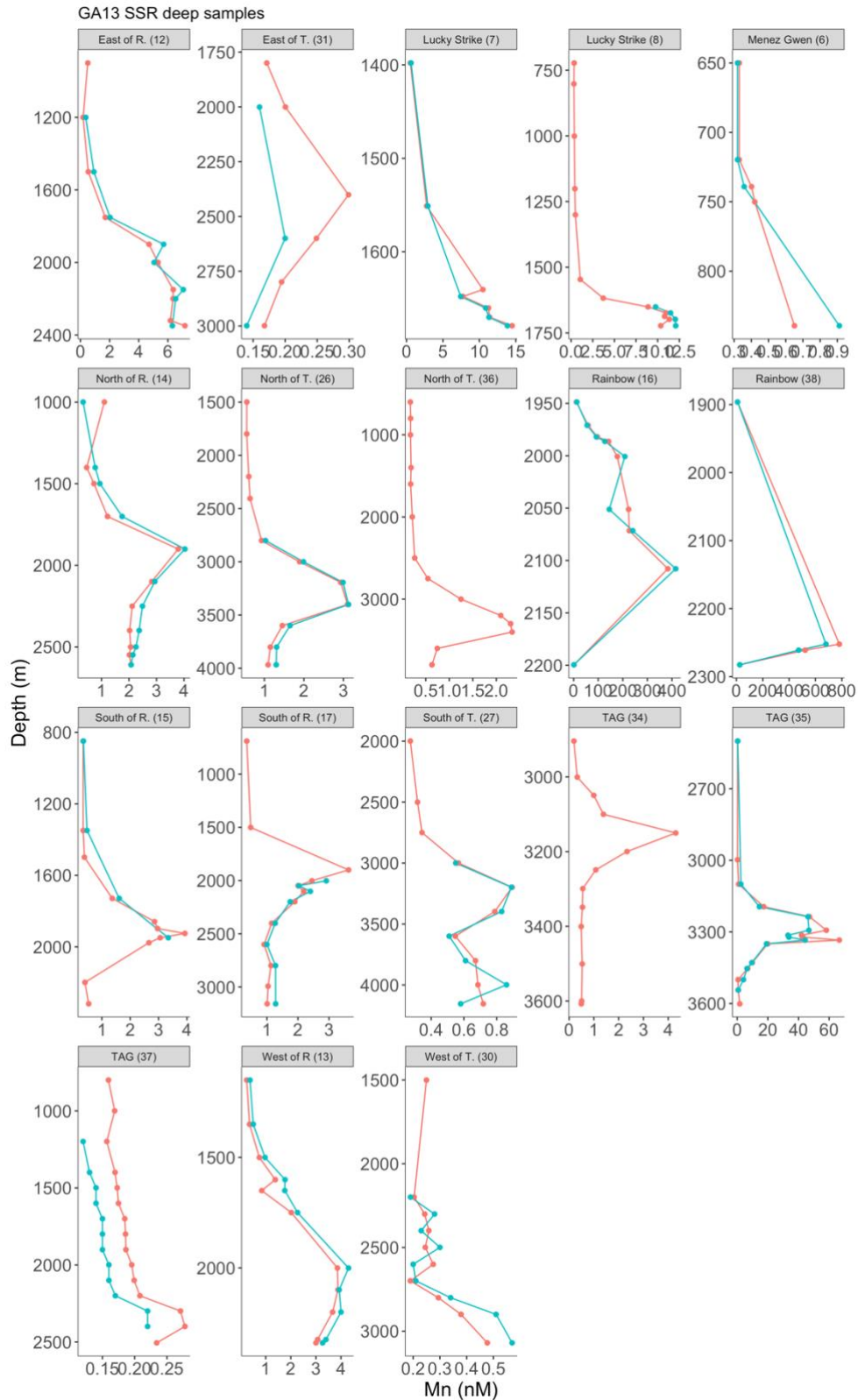


Figure S5. dMn (red) and TDMn (blue) data from the trace metal clean rosette at each station (grey box's), where dMn > 0.15 nM and dFe > 0.5 nM N. Atlantic background values and neutral density > 27 mg/kg. The dMn data is used with the slope values from Figure 4A to derive "xsHe_{Mn}" shown in Figure S5 and Figure 4. Main casts over vent sites are 6 = Menez Gwen, 7 and 8 = Lucky Strike, 16 and 38 = Rainbow, 35 and 36 = TAG.

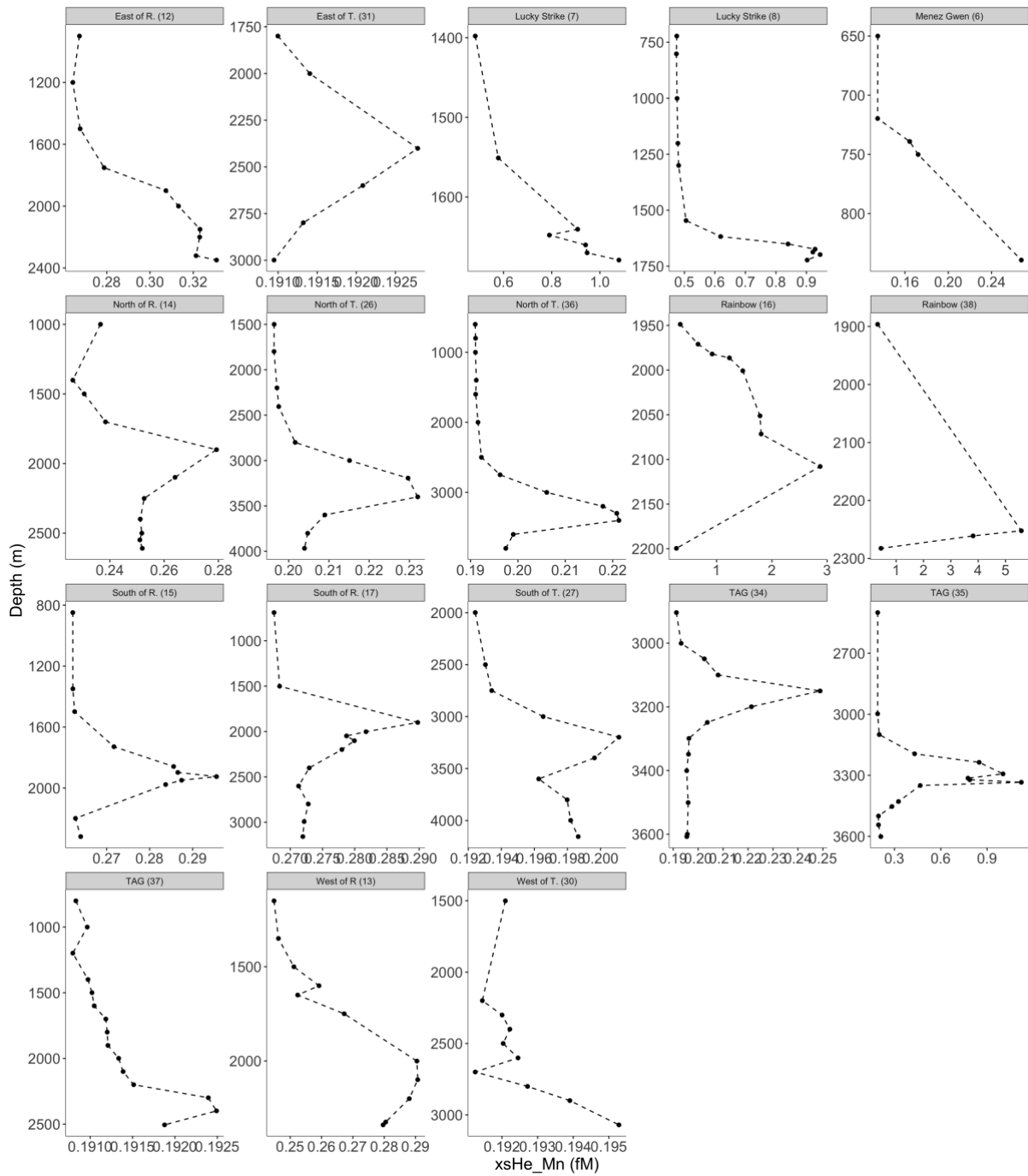


Figure S6. Derived xs^3He_{Mn} values for the trace metal clean rosette at each station (grey box's), where $dMn > 0.15$ nM and $dFe > 0.5$ nM N. Atlantic background value and neutral density > 27 mg/kg. The xs^3He_{Mn} data is calculated from the slope values shown on Figure 3A. Main casts over vent sites are 6 = Menez Gwen, 7 and 8 = Lucky Strike, 16 and 38 = Rainbow, 35 and 36 = TAG.

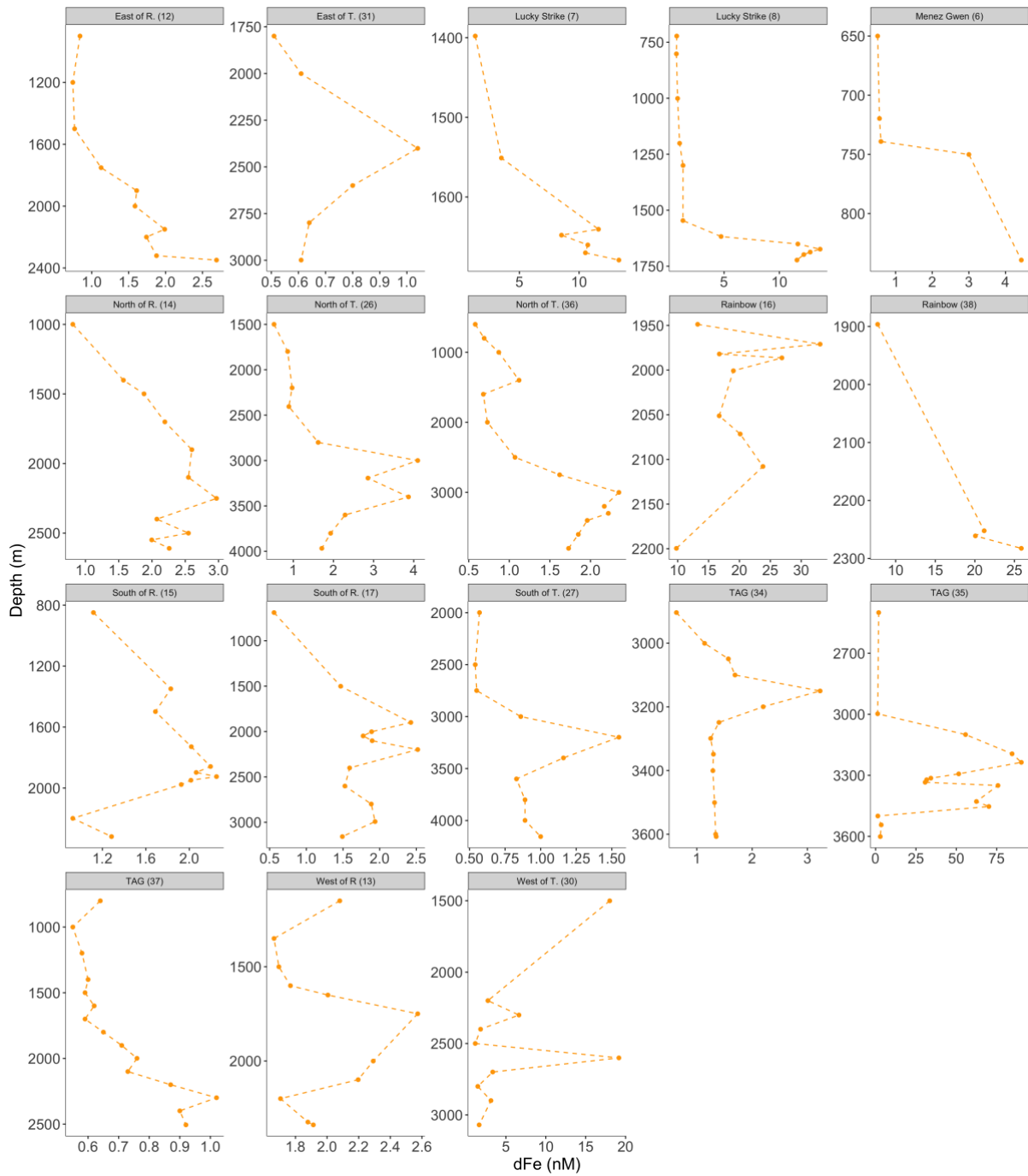


Figure S7. Dissolved Fe data (for the trace metal clean rosette) used for integration at each station (grey box's), where $dMn > 0.15$ nM and $dFe > 0.5$ nM N. Atlantic background value and neutral density > 27 mg/kg. Main casts over vent sites are 6 = Menez Gwen, 7 and 8 = Lucky Strike, 16 and 38 = Rainbow, 35 and 36 = TAG.

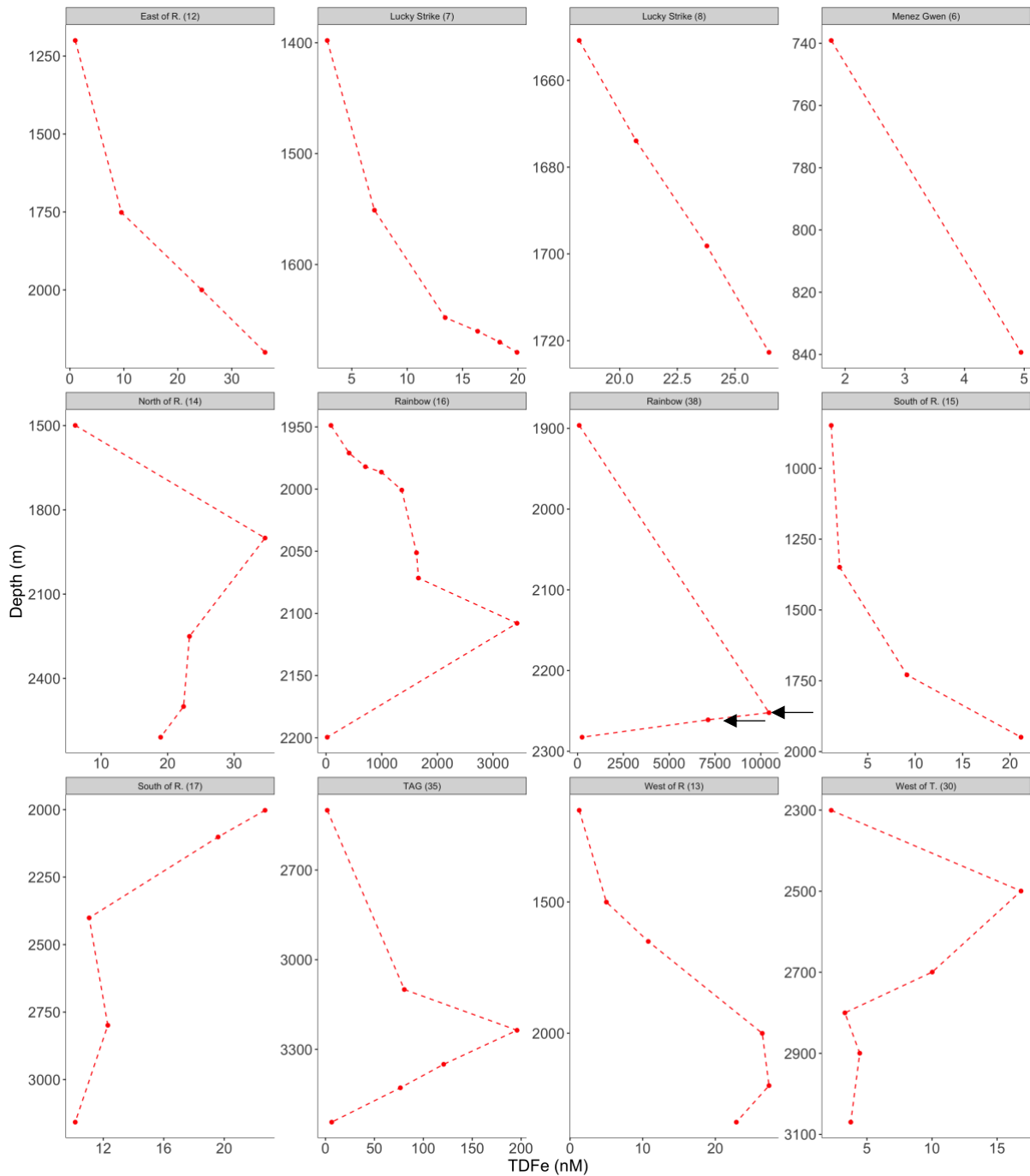


Figure S8. Total dissolvable Fe data (for the trace metal clean rosette) used for integration at each station (grey box's), where $dMn > 0.15$ nM and $dFe > 0.5$ nM N. Atlantic background value and neutral density > 27 mg/kg. Black arrows indicate young buoyant plume samples identified by high TDFe concentration, negative Eh, and ND anomaly (lower ND at same depth relative to background). These points were integrated separately (for sFe, dFe and TDFe) so as not to overestimate integrated values. Had more samples been collected between 2200 and 1900 m at station 38 we anticipate TDFe concentrations would of returned to the 1 – 1000 nM range observed at station 16. Main casts over vent sites are 6 = Menez Gwen, 7 and 8 = Lucky Strike, 16 and 38 = Rainbow, 35 and 36 = TAG.

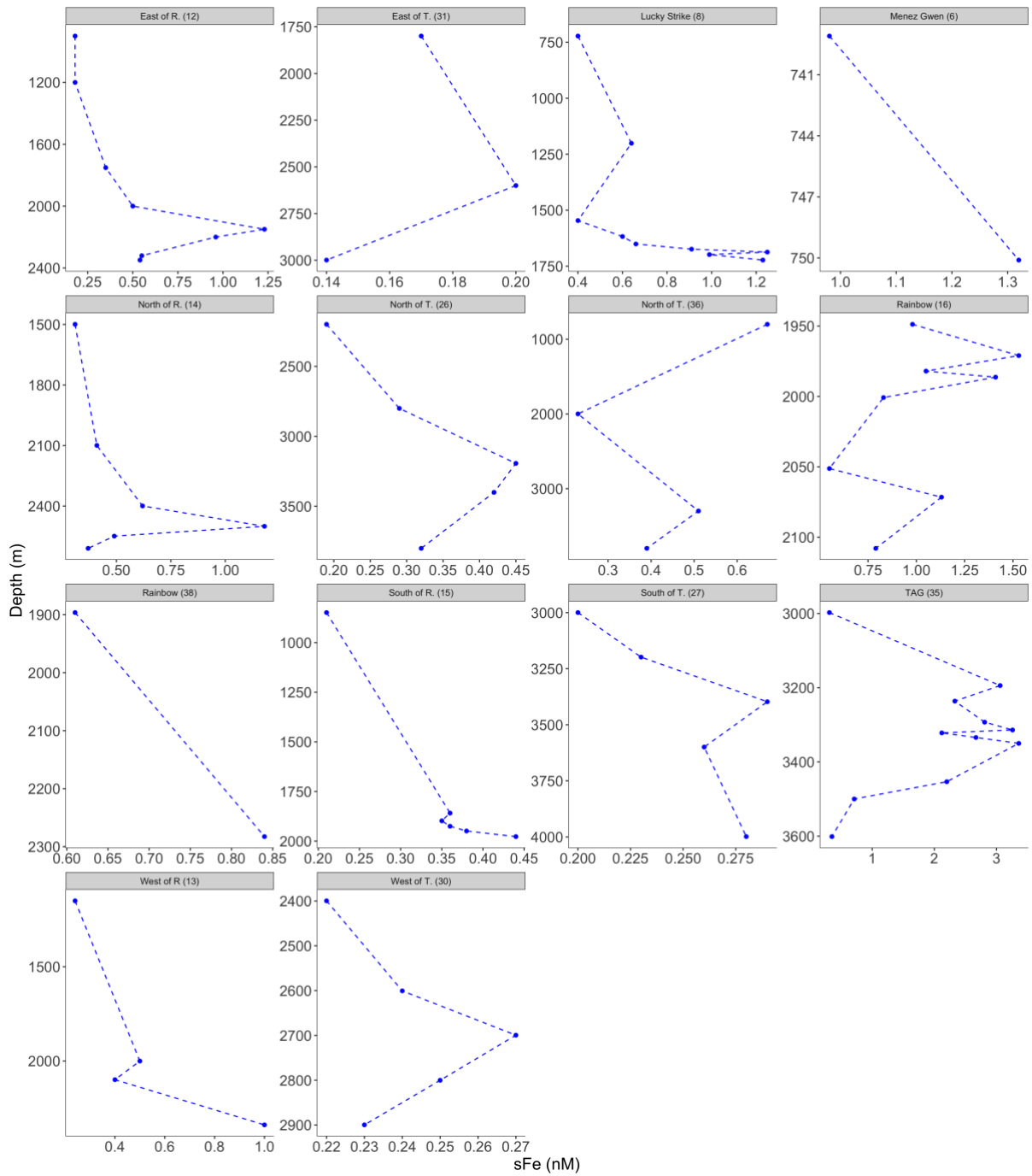


Figure S9. Soluble Fe data (for the trace metal clean rosette) used for integration at each station (grey box's), where $dMn > 0.15$ nM and $dFe > 0.5$ nM N. Atlantic background value and neutral density > 27 mg/kg. Main casts over vent sites are 6 = Menez Gwen, 8 = Lucky Strike, 16 and 38 = Rainbow, 35 and 36 = TAG.

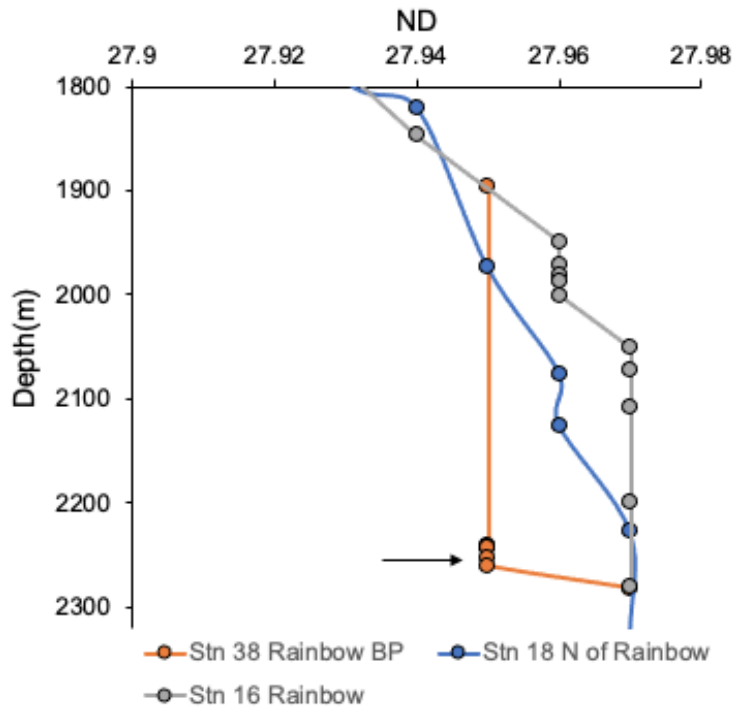


Figure S10. Comparison of neutral density (ND (kg/m^3)) profiles at 3 stations around Rainbow. The black arrow indicates samples from station 38 over Rainbow classified as being within the buoyant plume, as the density is lower than that of the other stations at the equivalent depth near the seafloor. These samples are the same as those highlighted by the black arrow in figure S7 that had the highest observed TDFe concentrations.

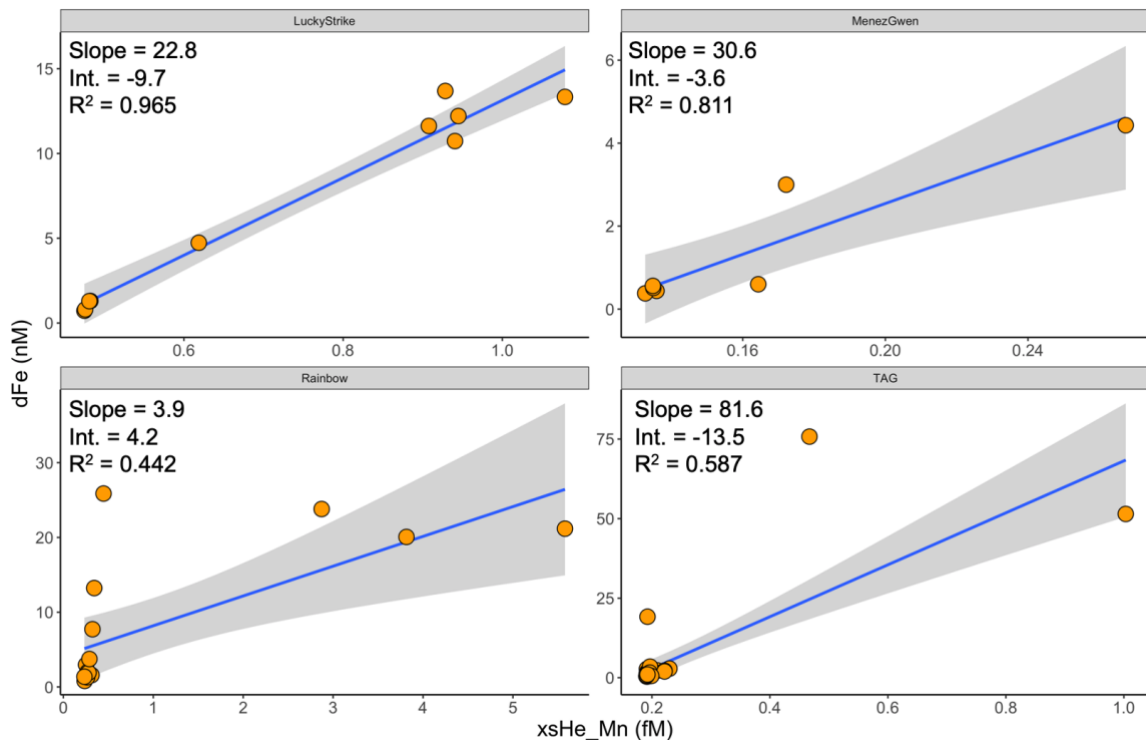


Figure S11. Linear regression statistics for $d\text{Fe}/x\text{s}^3\text{He}_{\text{Mn}}$ relationship at Lucky Strike (top left), Menez Gwen (top right), Rainbow (bottom left) and TAG (bottom right) using individual sample points (i.e. not integrated profiles as are the focus of the main text).

References

- Mellett, T., Albers, J., Wang, W., Lough, A. J. M., Santoro, A., Bundy, R. M., Lohan, M., Tagliabue, A., and Buck, K. N.: Particulate and dissolved iron exchange mediated by organic ligands in hydrothermal vent plumes along the Mid-Atlantic Ridge, in prep.
- Saito, M. A., Noble, A. E., Tagliabue, A., Goepfert, T. J., Lamborg, C. H., and Jenkins, W. J.: Slow-spreading submarine ridges in the South Atlantic as a significant oceanic iron source, *Nat. Geosci.*, 6, 775-779, 10.1038/ngeo1893, 2013.
- Vic, C., Gula, J., Roulet, G., and Pradillon, F.: Dispersion of deep-sea hydrothermal vent effluents and larvae by submesoscale and tidal currents, *Deep Sea Research Part I: Oceanographic Research Papers*, 1-51, 2018.